ORIGINAL PAPER

Diverse magma evolution recorded in trace element composition of zircon from Permo-Carboniferous rhyolites (NE German Basin, NW Polish Basin)

Elżbieta Słodczyk[1] · Arkadiusz Przybyło[1] · Anna Pietranik[1] · Réka Lukács[2,3,4]

Abstract

Permo-Carboniferous rhyolitic rocks are widespread in the NE German Basin and NW Polish Basin. Hafnium (Hf) and oxygen (O) isotopes analysed in zircon from these rocks suggest diverse sources and processes involved in the formation of rhyolitic magmas. In this study, detailed core-to-rim trace element compositions were analyzed in zircon from four localities that were previously analyzed for Hf and O isotopes. The trace element analyses, in particular Hf concentrations as well as Eu/Eu*, Ce/U, Yb/Gd, and Th/U ratios, are consistent with prolonged magma evolution in three localities from the NE German Basin (Fehmarn, Slazwedel and Penkun). The fourth locality within the NW Polish Basin (Wysoka Kamieńska) is consistent with a shorter period of magma evolution. Similar stages were distinguished in zircon from the three NE German Basin localities that include: early crystallization followed by rejuvenation with more primitive magma (stage A), subsequent fractional crystallization (stage B) and finally late crystallization in a saturated system or alternatively late rejuvenation with a more primitive magma (stage C). Interestingly magmatic rims on inherited zircon grains have compositions typical for late stage B and stage C, which is consistent with their late addition to evolving rhyolitic magma, most probably during assimilation and not during source melting. The zircon from the fourth, NW Polish Basin locality shows limited compositional variability consistent with the eruption of hot magma not long after the zircon started crystallizing. Thus trace element analyses in zircon provide a record of magmatic processes complementary to that of Hf and O isotope analysis, in that, a detailed analyses of core-to-rim compositional variations are particularly useful in distinguishing respective stages of magma evolution and can pinpoint the relative timing of inherited grains being incorporated into magma.

Keywords Trace elements · Isotopes · Zircon · Magma differentiation · AFC · Inherited grains · Permo-Carboniferous volcanism

Introduction

Accessory minerals such as zircon, apatite, and titanite, despite constituting usually less than 1% of the rock volume, can control the trace element budget of a magma (e.g. Rivera et al. 2014; Yan et al. 2020; Lukács et al. 2021). This is because they contain an abundance of many trace elements. Consequently, the composition of accessory minerals represents trace element variations for an evolving magmatic system experiencing the coeval crystallization of variable minerals. In particular, zircon may record crystallization processes and contemporaneous changes in composition and temperature of its host melt in its textural, trace element, and isotopic composition (e.g. Bindeman et al. 2008; Stelten et al. 2015; Deering et al. 2016; Reid and Vazquez 2017). This, combined with zircon's resistance to alteration

✉ Elżbieta Słodczyk
elzbieta.slodczyk@uwr.edu.pl

1 Institute of Geological Sciences, University of Wrocław, Pl. M. Borna 9, 50-204 Wrocław, Poland

2 Institute for Geological and Geochemical Research, Research Centre for Astronomy and Earth Sciences, ELKH, Budaörsi út 45, Budapest 1112, Hungary

3 CSFK, MTA Centre of Excellence, Konkoly Thege Miklós út 15-17, Budapest 1121, Hungary

4 MTA-ELTE Volcanology Research Group, ELKH, Pázmány P. sétány 1/C, 1117 Budapest, Hungary

and dissolution makes it a valuable fingerprint of magmatic conditions, particularly when information from cogenetic mineral phases have been obliterated. This is often the case in volcanic rocks, where the original composition has been changed by alteration due to weathering at the Earth's surface and/or metasomatic processes.

In this contribution, we investigate the potential of zircon to record magma evolution by tracking core-to-rim trace element concentrations to reveal changes in melt chemistry through time, focusing on both magmatic and inherited grains. In the case of the latter, the concept of the magmatic rim on inherited grain is introduced. We hypothesize that careful comparison of the composition of such rims with that of magmatic grains will provide information on the timing of an inherited grain's incorporation into the evolving silicic magma. This study focuses on zircon grains from four occurrences of high-silica volcanic rocks formed during the post-Variscan magmatic flare-up in central Europe. The zircon grains were analyzed for Hf and O isotopes and were then interpreted in the context of magma mixing and/or partial melting of diverse sources (Pietranik et al. 2013). The isotopic and trace element records are combined in this study.

Geological setting

In central Europe, the late Carboniferous and early Permian represent a period of change in the tectonic regime, from compressive to extensional/transtentional (e.g. McCann et al. 2006). Rift basins formed and provided the pathways for magmas and voluminous silica-rich volcanism (Benek et al. 1996; Van Wees et al. 2000). The widespread SiO_2-rich magmatic activity formed various (sub-) volcanic edifices, such as large caldera systems with voluminous pyroclastic deposits and porphyry stocks, laccoliths, and resurgent domes. Depending on the location of the magmatic centres (either within intramountain basins, on Variscan and Cadomian basement, or its foreland), the lithological and emplacement record of these volcanics varies. Permo-Carboniferous volcanism typically occurred in laccolith-/sill-/dome-systems that are often emplaced within a basin's thick sedimentary succession (e.g. Saale Basin with rhyolitic laccoliths of the Halle Volcanic Complex; Mock et al. 2003; Schmiedel et al. 2015; Fig. 1). On the other hand, extensive and thick sheets of welded ignimbrite with high explosivity centres are found on the eastern part of the Variscan Belt in Europe (e.g. calderas of the North Saxon Volcanic Center, Hübner et al. 2021; Repstock et al. 2018; or the Altenberg-Teplice, Casas-García et al. 2019, 2021; Fig. 1); whereas a wide range of possible morphological volcanic forms occurs within the voluminous magmatism of the Central European Variscan foreland surrounded by the (SPB) Southern Permian Basin (e.g. Benek et al. 1996; Paulick and Breitkreuz

2005; Geißler et al. 2008; Maliszewska et al. 2016). The time of the formation of the SPB was accompanied by extensional activity, strike-slip movements, and thermal relaxation that allowed large-scale magmatism to occur (Van Wees et al. 2000). As time went by, the SPB volcanics were covered by a thick pile of sediments. The present state of the art concerning these volcanics is based on hundreds of hydrocarbon wells reaching a depth of 8 km (Breitkreuz and Kennedy 1999; Geißler et al. 2008). The products of this volcanic activity extend over an area of ca. 160,000 km^2 and their drilled thickness reaches up to 2000 m. The textural differences between these volcanic deposits allowed for the distinction between welded ignimbrites, lava flows, domes, and subvolcanic bodies (Geißler et al. 2008; Maliszewska et al. 2016). This paper focuses on the silicic (dacitic to rhyolitic) lavas and ignimbrites within the central part of the SPB, that is the Northeast German Basin (NEGB) and the Northwest Polish Basin (NWPB; Fig. 1b).

Previous studies on Permo-Carboniferous rhyolites within the Northeast German Basin (NEGB)

The estimated volume of the NEGB is ca. 48,000 km^3 and comprises five successive eruptive stages (andesitic > ignimbritic > post-ignimbritic > late rhyolitic > basaltic; Benek et al. 1996). While Geißler et al. (2008) recognized seven main volcanic products within the German part of the SPB, from which (1) SiO_2-rich lava flows, lava domes, laccoliths and (2) SiO_2-rich ignimbrite sheets (welded and nonwelded) were dominating, with subordinate (3) basaltic to andesitic shield volcano complexes, with (4) pyroclastic deposits related to the eruption of lava domes; (5) smaller basaltic and andesitic lava fields, (6) basaltic to andesitic sill complexes, and (7) volcanoclastic sediments. The rhyolitic rocks of the NEGB analyzed in this study are from the lava-dominated region which is represented by investigated drill cores of Fehmarn, Penkun, and Salzwedel (Fig. 1b). The SHRIMP zircon U–Pb age determination of silicic volcanics within the investigated region showed: (1) synchronicity of the magmatic activity focused between 295 and 299 Ma, and (2) variable proportions and ages of inherited grains between investigated drill cores (Breitkreuz and Kennedy 1999; Breitkreuz et al. 2007; for the summary of magmatic and inherited zircon ages used in this paper see Table 1). Further insight into the magmatism of this region was provided by Pietranik et al. (2013) who revealed two stages in the silicic magma evolution based on zircon composition. Within the growth zones of zircon of magmatic origin, two successive stages were identified with distinct characteristics, suggesting successive crystallization environments. These two stages were recorded in zoned and unzoned crystals. The first magmatic stage was recognized in high Zr/Hf zircon cores and refers to a less differentiated magma
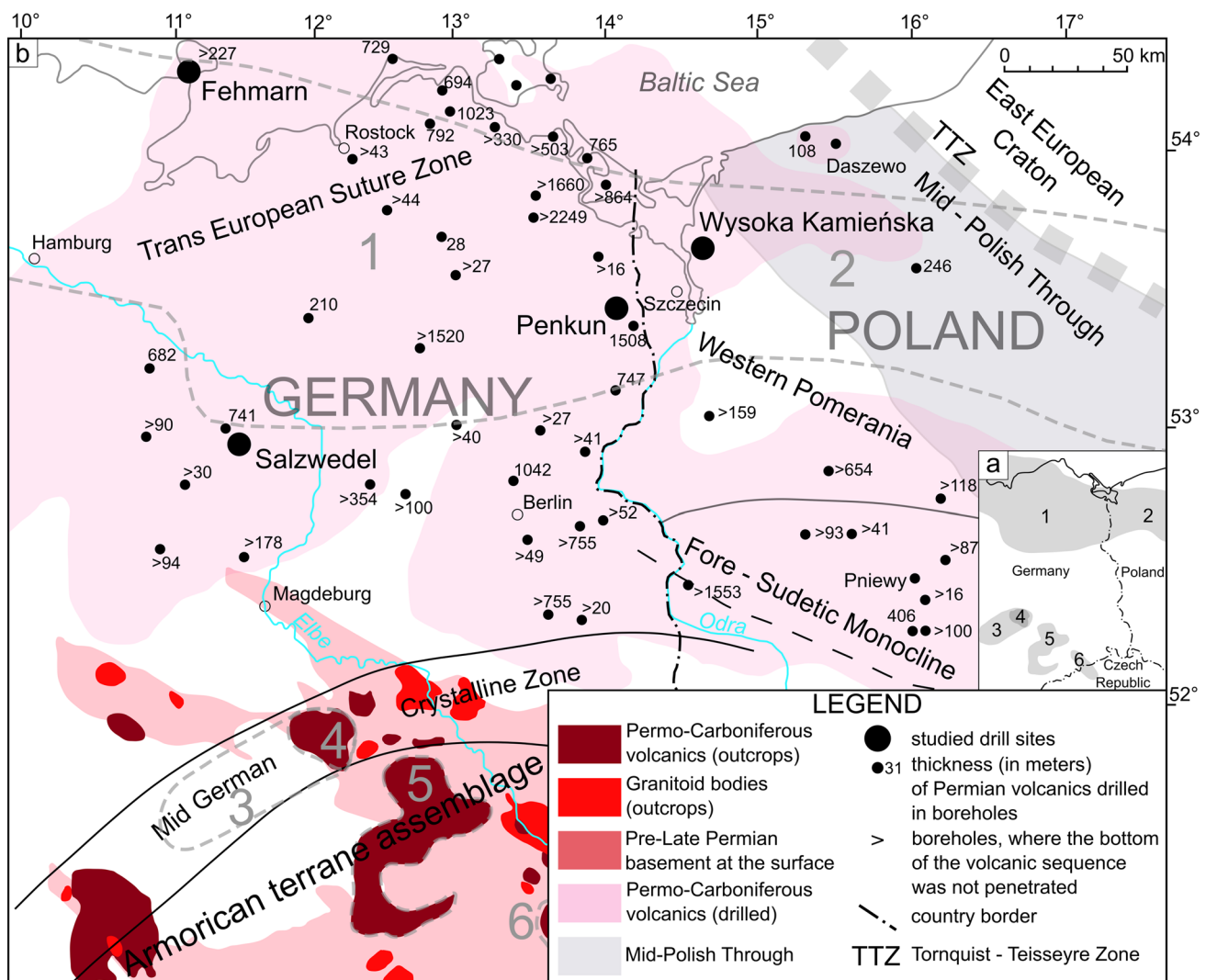
Fig. 1 Map of Permo-Carboniferous rhyolites within the NE German Basin and the NW Polish Basin showing the investigated sampling sites; **a** numbers refer to the respective regions: 1—NE German Basin, 2—NW Polish Basin, 3—Saale Basin, 4—Halle Volcanic Complex, 5—North Saxony Volcanic Complex, 6—Altenberg–Tep-lice Complex; **b** numbers refer to the thickness of drilled volcanic rocks in meters (data from Dadlez 2006, Geißler et al. 2008). Map modified after compilation from Dadlez (2006), Breitkreuz et al. (2007), Geißler et al. (2008)

composition (recorded as a wide range of Hf and O isotope compositions—for an isotopic summary see Fig. 2; higher Th/U ratios; lack of correlation between Zr/Hf vs Th/U and Y vs P). The zircon at this first stage crystallized from heterogeneous, compositionally distinct magma pulses in small, unrelated magma portions that reflect either various sources or combined crustal assimilation and fractional crystallization processes with an estimated juvenile component involved in the magma generation from 5 to 80%. The following second stage was recorded as having low Zr/Hf zircon rims in zoned grains (while unzoned grains showed a constant low Zr/Hf concentration throughout the inner part and rim of the grain) and refer to a more fractionated and differentiated composition (recorded as lower Th/U ratios;

the correlation between P vs Y; the small range of Hf and O isotope compositions). Zircon from this stage crystallized in a well-mixed (homogeneous) magma body with an estimated juvenile component involved in this magma generation varying from 30 to 40% (Pietranik et al. 2013).

Previous studies on Permo-Carboniferous rhyolites within the Northwest Polish Basin (NWPB)

The drilling record of volcanic, subvolcanic, and volcanogenic rock thickness indicates a volumetric decrease of these rocks from the NEGB toward the NW Polish Basin (NWPB). The lower Permian rocks of the western part of the NWPB also come from cores of deep boreholes and

Table 1 Summary of the previous study done on zircon grains from Permo-Carboniferous rhyolites studied in this paper

	Penkun [highly plag-Kfsp-phyric dacite]	Salzwedel [porphyritic rhyolite]	Fehmarn [Fsp rich porphyritic rhyolite]	Wysoka Kamieńska [Fsp rich porphyritic rhyolite]
	Magmatic zircon			
Age (Ma) [1]	295–312 ($n=10$)	286–296 ($n=8$)	290–298 ($n=10$)	286–300 ($n=15$) 302 ± 1.5[b] (n=16)
$\delta^{18}O$ (±2σ=0.6) [2]	7.6–9.6 ($n=10$)	7.5–9.4 ($n=8$)	6.2–8.0 ($n=9$)	6.2–7.7[b] ($n=19$)
εHf [a][2]	− 4.1 to − 8.3 (n=7) (±2σ between 0.7 and 0.9)	− 5.3 to − 7.7 (n=5) (±2σ between 0.7 and 1.1)	− 0.6 to − 7.3 (n=9) (±2σ between 0.7 and 1.1)	− 5.6 and − 7.7[b] (n=12)
Depleted mantle Hf modal age [2]	1619, 1534, 1526, 1707, 1566, 1514, 1450	1573, 1531, 1523, 1563, 1666,	1417, 1161, 1507, 1539, 1577, 1529, 1645, 1566, 1501	–
	Inherited zircon			
Age (Ma) [1]	1793, 1464, 1665, 567, 567,	800, 982, 1440, 774, 1183, 1393, 2104, 1564	317, 317, 1078, 1390, 485, 1446,	Inherited grains not detected by [1] 355.5 ± 5.1[b]
$\delta^{18}O$ (±2σ=0.6)[2]	5.9–9.3	6.2–8.9	6.0–9.1	–
εHf [a][2]	5.3; 0.9; 18.9; − 7.2 (±2σ between 0.6 and 1.1)	− 20.3; 0.0; − 7.1; − 2.7; 2.0; 1.1; 3.6	− 4.2; − 4.2; 0.4; − 1.8; 6.8; 1.3 (±2σ between 0.5 and 0.9)	–
Depleted mantle Hf modal age [2]	2066, 2074, 1852	2829, 1745, 2547, 1745, 1784, 2005, 1989	1473, 1471, 1799, 2181, 933, 2038	–

[1] Breitkreuz et al. (2007), [2] Pietranik et al. (2013)

[a]Some grains were not analyzed; for respective measurements within particular zircon grains see Table 1 in [2]

[b]Zircons analysed by Słodczyk et al. (2018) from the same drill core, from neighbouring sample to that dated by Breitkreuz et al. (2007); only one older grain found out of 31 grains
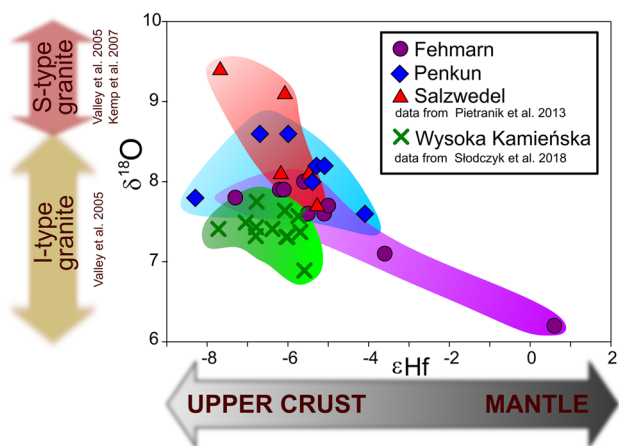

Fig. 2 Summary of previous studies on rhyolitic zircon characterized by variable oxygen and hafnium isotopic composition. The rhyolites represent Permo-Carboniferous magmatism within the NE German Basin and the NW Polish Basin (data from Pietranik et al. 2013; Słodczyk et al. 2018, respectively). The very same zircon grains from Penkun, Salzwedel, and Fehmarn were analyzed in this study, while Wysoka Kamieńska represents the very same drill core and rock record with isotopic and trace element analyses done on zircon from a neighbouring depth

rocks are covered by younger sediments of approximately 1000–5000 m thickness, increasing towards the Teisseyre-Tornquist Zone (Karnkowski 1999; Maliszewska et al. 2016). The NWPB belongs to two regional units, the Fore-Sudetic Monocline, and the western Pomerania, with a volumetric predominance of acidic over intermediate rocks within the latter. The volcanic rocks from the Fore-Sudetic Monocline consist mainly of andesites and trachyandesites, with minor rhyolites, dacites, trachytes, and local basalts (Jackowicz 1995). Regarding pyroclastic rocks, silicic ones are relatively thin but more common compared to ones of intermediate composition. The volume of these explosive deposits is exceeded by subvolcanic and plutonic rocks comprising variable proportions of microdiorites, micromonzonites, microgranitoids, granites, syenites, gabbros, trachyandesites, andesites, and trachytes (Maliszewka et al. 2016; Żelaźniewicz et al. 2016). Contrastingly, western Pomerania is dominated by rhyolites and dacites with subordinate trachyandesites, andesites, and trachytes (Jackowicz 1995). Silicic pyroclasts are frequent but not voluminous and subvolcanic rocks are represented by microdiorite and micromonzonite. Units of the NWPB were exposed to three stages of alteration (e.g. carbonatization, albitization, hematitisation, sericitization, impregnation by sulphates or illitisation in perlitic rocks) which can be linked with (1) volcanic exhalations and hot springs, (2) circulation of warm pore waters during

present a succession from tens of centimetres to over 350 m (not all boreholes cover the whole section). The volcanic

progressive burial and (3) very low-grade metamorphism (Maliszewska et al. 2016). Alteration can obfuscate regional correlations. However, the western part of the SPB was affected by much more intense volcanism than the eastern part. The zircon U–Pb ages of the NWPB "flare-up" silicic magmatism were determined by SHRIMP (293.0 ± 2.3 to 298.5 ± 3.3 Ma, Breitkreuz et al. 2007) and SIMS (297 ± 3 to 301 ± 5 Ma, Słodczyk et al. 2018). Zircon from those silicic rocks lacks inherited cores (for details see Table 1). The western Pomerania late Palaeozoic rocks are dominated, volumetrically, by silica rich lavas, that in turn may indicate a greater impact on the crustal environment compared to the mafic-dominated Fore-Sudetic Monocline. This may further indicate a lower proportion of evolved crustal components to the mantle source in the latter. The Fore-Sudetic Monocline shows larger lateral and lower vertical variability of petrochemical indicators compared to the western Pomerania, which reflects not only different intensities and proportions of melted source material (variable degree of contamination) but also spatial diversity in the composition of this source material (Maliszewska et al. 2016). This diversification of the source material for these late Palaeozoic magmas was confirmed in different proportions of zircon ages (inherited or magmatic) and their O and Hf isotope signatures indicating a derivation of magma from a sedimentary source (Carboniferous turbidites with an admixture of Baltica and/ or Avalonia component) for the Fore-Sudetic Monocline rhyolites and an antagonistic mixture of fine-grained sedimentary material with mantle-derived magmas for the west Pomerania rhyolites (Słodczyk et al. 2018).

Previous studies on zircon from the studied area

Zircon analyzed as part of this research represents Permo-Carboniferous silicic volcanics from 4 drill cores (samples Penkun, Salzwedel, and Fehmarn of the NEGB and

Wysoka Kamieńska of the NWPB, see Fig. 1). These grains were first handpicked from crushed rock, mounted and dated (Breitkreuz et al. 2007), followed by O and Hf isotopic determination for representative grains (Pietranik et al. 2013). The whole rock composition of the studied rocks was not analyzed, but we refer to literature data for rhyolites located in the studied areas (Benek et al. 1996; Żelaźniewicz et al. 2016). The Rare Earth Element (REE) normalized diagrams for these rocks show considerable uniformity in composition (Fig. 3a). However, the samples in this study were chosen due to their diversity in isotopic composition (see Fig. 2) as well as the proportion of magmatic-to-inherited zircon grains (Penkun = 2.6; Fehmarn = 3.0; Salzwedel = 0.7; Wysoka Kamieńska = 0.0; data from Pietranik et al. 2013). The choice of the very same zircon grains for analyses was determined by their diversity and the possibility to correlate the new trace element data with already known isotopic differences (Pietranik et al. 2013). The samples represent sections of the following four drill cores described by Breitkreuz et al. (2007): (1) *Penkun* (1/71 drill core): ~ 450 m thick highly Pl-Kfs dacite lava, (the bottom not penetrated), sampling depth 4690 m; (2) *Salzwedel* (2/64 drill core): porphyritic rhyolitic lava dome of almost 700 m thickness, sampling depth 4150 m; (3) *Fehmarn* (Z1 drill core): porphyritic rhyolitic lava dome with large Fsp phenocrysts with a minimum thickness of 160 m (the bottom not penetrated), sampling depth 194 m; (4) *Wysoka Kamieńska* (listed there as Wysoka Kamieńska-2 drill core): porphyritic rhyolite lava flow with Fsp phenocrysts < 0.5 cm; the thickness reaching 480 m, with the bottom drilled through at a depth of 3500 m), sampling depth 3500 m.
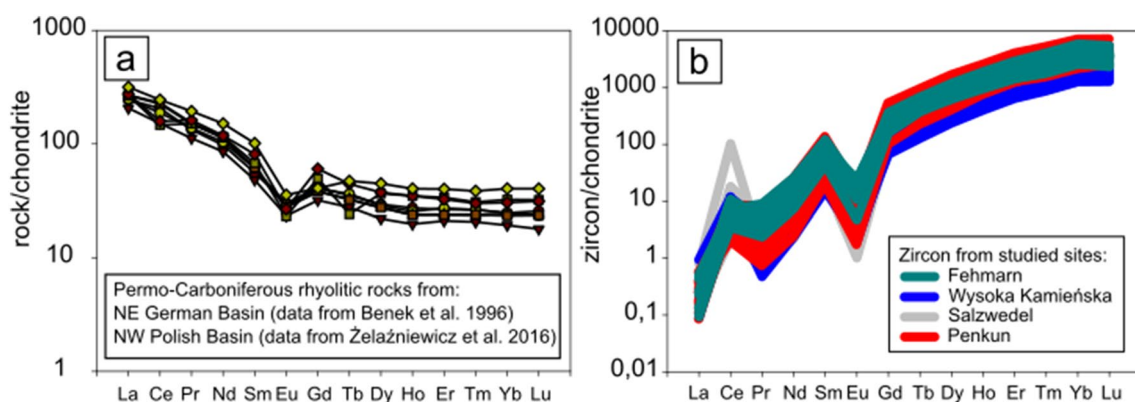

Fig. 3 Rare Earth Element normalized patterns for **a** rhyolitic whole rocks, data from Benek et al. (1996) for the NE German Basin and from Żelaźniewicz et al. (2016) for the NW Polish Basin; **b** zircon analyzed in this study. Data normalized to chondrite after Anders and Grevesse (1989)
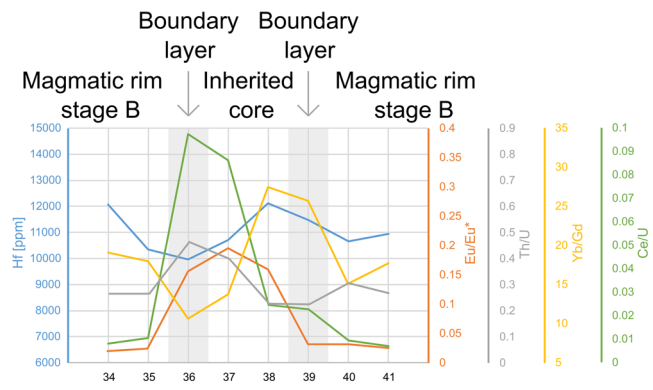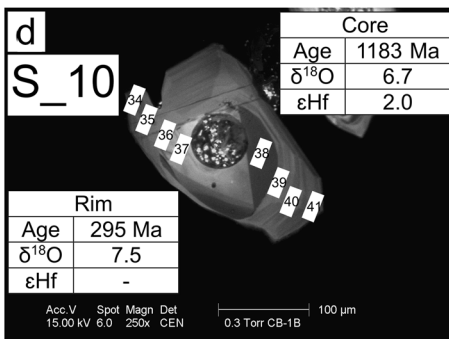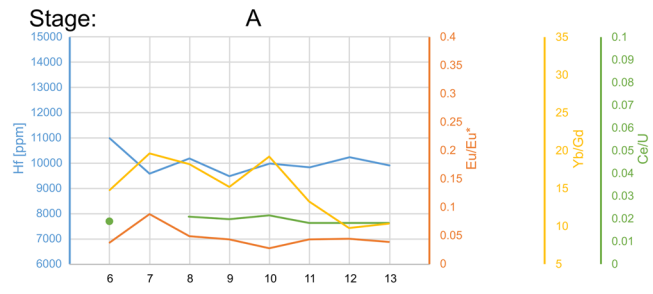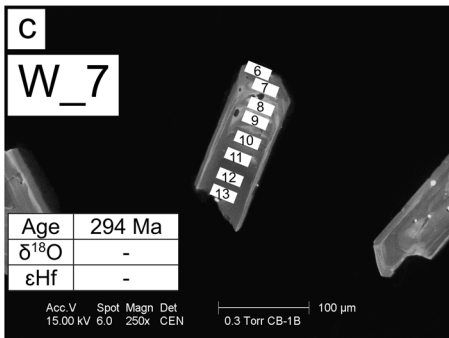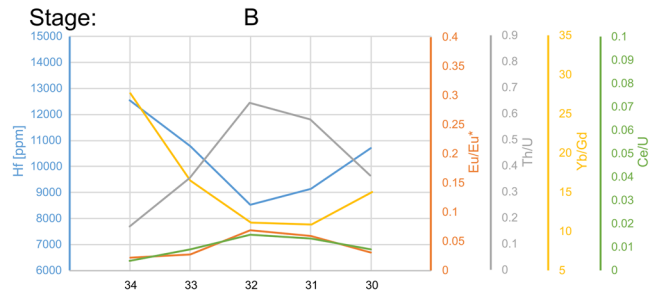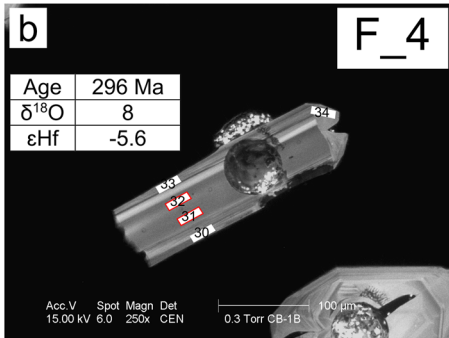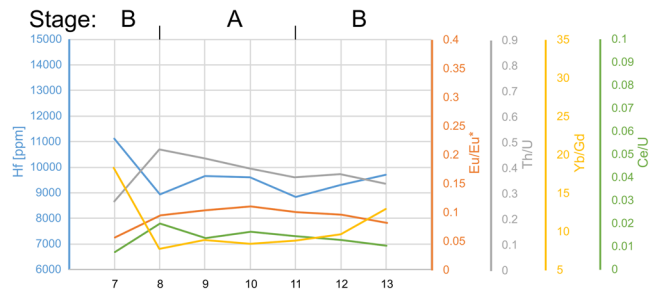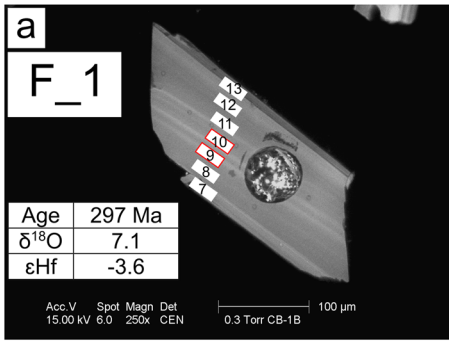
◄**Fig. 4** Cathodoluminescence (CL) images and complementary trace element core-rim traverses across exemplary zircon grains; **a** oscillatory zoned magmatic zircon with complex compositional zonation; **b** oscillatory zoned magmatic zircon with simple compositional zonation pattern; **c** oscillatory zoned magmatic zircon showing minimal compositional zonation; **d** inherited grain with marked boundary layer and following magmatic rim. The rectangles show analytical spots, with corresponding analyses shown on the right hand side graphs; the red rectangles indicate analyses correlated with isotopic data. The given age is from Breitkreuz et al. (2007), while the isotopic composition is from Pietranik et al. (2013). For the whole documentation of investigated zircon grains see Supplementary Materials 1–5

Methods

Selected trace elements were investigated in both magmatic and inherited zircon grains, that are surrounded by a magmatic rim, previously investigated by Breitkreuz et al. (2007) and Pietranik et al. (2013). Thus, the following ratios of magmatic to inherited zircon grains were under scrutiny from drill cores at Penkun (13/5 grains), Salzwedel (6/10 grains), Fehmarn (13/5 grains), Wysoka Kamieńska (10/no inherited grains). The Wysoka Kamieńska sample was the only one not previously investigated for zircon O and Hf isotope composition by Pietranik et al. (2013). However, zircon O and Hf isotope composition from a neighbouring sample in the same drill core was documented by Słodczyk et al. (2018). Trace element compositions were measured in zircon previously analyzed by Pietranik et al. 2013. While previous data (including Zr, Hf, U, Th, Y, and P concentrations) were reanalysed for Y, La, Ce, Pr, Nd, Sm, Eu, Gd, Tb, Dy, Ho, Er, Tm, Yb, Lu, Hf, Th, and U elements as part of this study. We checked and confirmed that the Zr/Hf ratio and Hf concentration range and patterns through the same zircon zones are consistent with the results by Pietranik et al. (2013). However, our results and discussion refer only to the newly measured trace element data with a higher measurement density to track Hf versus other elements variations for the same analytical spots (Appendix 1, Supplementary Materials 1–5). Compilation of the new trace element data with O and Hf isotopic composition uses the same path as presented in Pietranik et al. (2013), where isotopic data were juxtaposed together only with the results from the neighbouring trace element spot, localized within the same zircon zone (Fig. 4 and Supplementary Materials). Trace and rare earth element (REE) concentrations in zircon were analyzed using an Element 2 ICP-MS (Thermo Fisher Scientific) coupled with an Analyte Excite 193 nm excimer laser ablation system (Teledyne/Cetac) at the Institute of Geology of the Czech Academy of Sciences, Prague. Linear rasters of 16 μm beam size, 40 μm raster length, and 2 μm/s scan speed were ablated alongside the growth zones in zircon grains. Samples were ablated using a repetition rate of 10 Hz and laser fluence of 3 J/cm^2. Calibration and reference standards (glasses

NIST 612, NIST 610, and zircon 91,500) were measured regularly after every 10 samples. Each analysis included the acquisition of 15 s gas blank and 20 s laser ablation signal. The time-resolved signal data were processed using the Glitter software (Van Achterbergh et al. 2001). NIST 612 was used for the calibration of element concentrations and the isotope ^{29}Si was used as an internal standard assuming its concentration based on zircon stoichiometry.

Results

The selection of grains for trace element studies was based on cathodoluminescence (Fig. 4 and Supplementary Materials: SM 1–5). The grains were often well preserved pyramidal in shape, sometimes the grains were fragmented (see SM 1–5). Where possible, grains were analyzed in full traverses from rim to rim, with up to eleven spots per grain. Zircon from all four locations show magmatic zonation expressed by both fine and/or thick oscillatory zoning (Fig. 4a–d). The REE pattern is also typical for magmatic grains (Fig. 3b). Resorption surfaces within magmatic grains are rarely seen and visible only in some grains (e.g. grain F_13 in SM 2), whereas more often than not such surfaces are present on inherited cores (Fig. 4d). Both elongated and stubby magmatic grains are observed in all locations, with a general minor predominance of the latter.

The whole set of data for the magmatic zircon grains presents similar trends for Hf, Yb/Gd, Th/U, Eu/Eu*, and Ce/U (Fig. 5). The pattern for Hf concentration and Yb/Gd ratio behave similarly, whereas Th/U ratio has an opposite direction to the trend. The Eu/Eu* and Ce/U trends are usually similar (Figs. 4 and 5). The typical pattern moving from core to rim is of increasing Hf and Yb/Gd, while Th/U and Eu/Eu* decrease. However, for some grains the pattern in the core region is more complex, and is characterized by either constant or decreasing Hf. In the following description we, therefore, distinguish between cores (constant or decreasing Hf) and rims (increasing Hf). Furthermore, the outermost rims show no consistent change in compositional trends characterized by either a decrease, increase or stabilization of Hf content. Similar patterns can be seen in all studied localities, but each locality also has its own characteristic pattern (e.g. the same pattern but different ranges of analyzed indices).

Zircon from Fehmarn

We analyzed 18 zircons of which five were inherited with magmatic rims. Magmatic zircon from Fehmarn cover the broadest ranges of analyzed indices among investigated sites. In detail, the magmatic zircon grains are characterized by the following composition (Fig. 6): Hf (8000–13,000 ppm), Eu/

Fig. 5 Generalized example of core-to-rim trace elements trend. The presence of particular fragments of this general trend in individual localities and grains is indicated. Additional information about magmatic rims on inherited zircon grains is also included. For detailed information see results and discussion
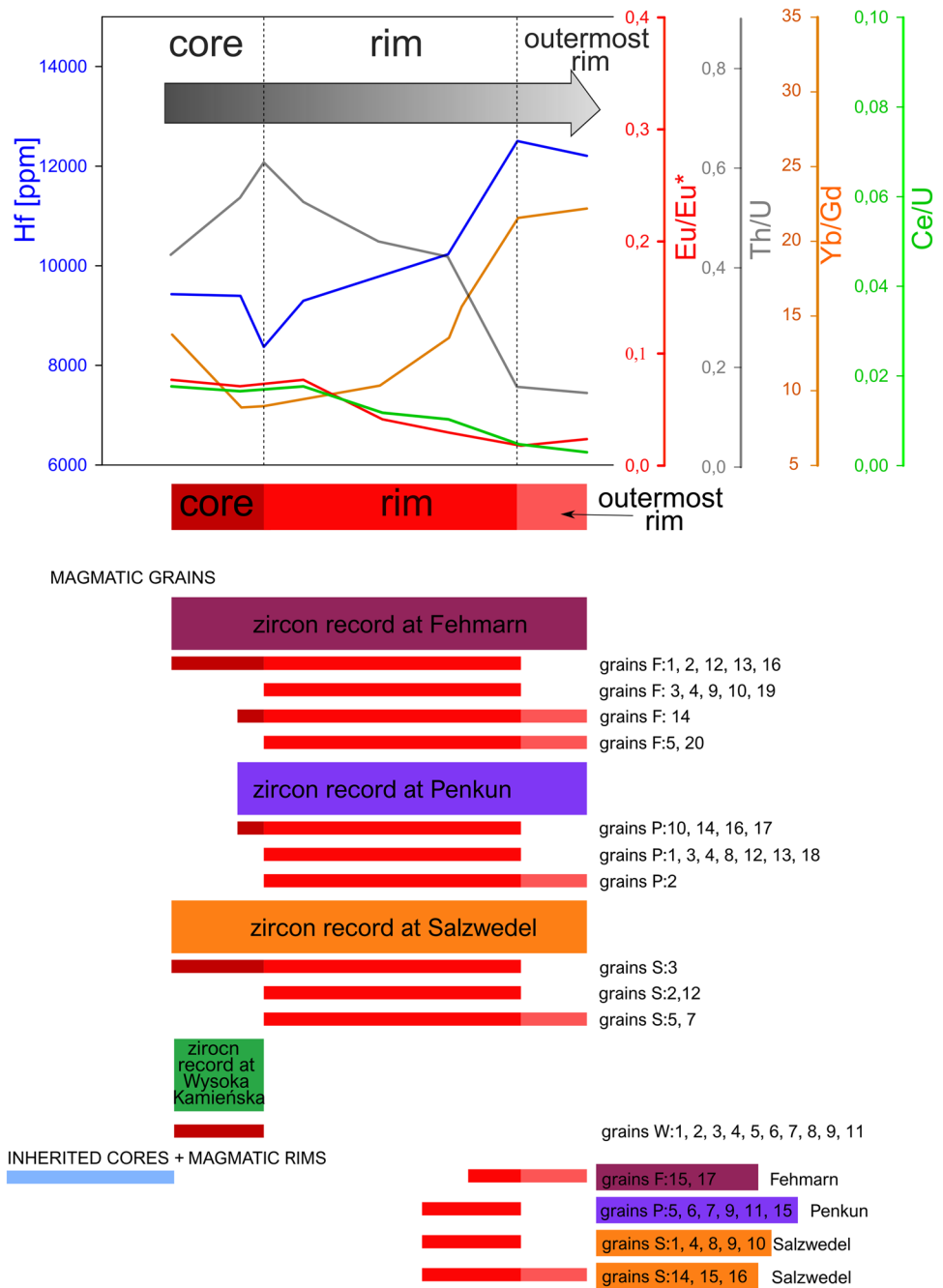
Eu* < 0.15, Th/U (0.1–0.7), Yb/Gd (7–35), and Ce/U < 0.04. Correlation between trace elements and Hf and O isotopic composition (Fig. 7) shows that: (1) the core is characterized by variable δ^{18}O from 6.2 to 7.8 ‰ and εHf from − 7.3 to 0.6, and both isotopic systems show some correlation with Eu/Eu*, (2) the rim shows a very narrow range of O and Hf isotopic composition (δ^{18}O 7.6 to 8 and εHf – 6 to − 5) accompanied by relatively large variations in trace element composition compared to the core. The five inherited grains have ages of 1446 Ma, 1390 Ma, 1078 Ma, 485 Ma, and 317 Ma (cf. Breitkreuz et al. 2007 and Table 1) measured

within rounded cores distinguished on CL images (for all documentation see SM 1 and 2). Trace element concentrations for these inherited grains have varied ranges, generally much more variable than the ranges for magmatic grains (Fig. 8). Magmatic rims on these inherited zircon grains were observed on all 5 grains, with doable measurements within 4 of them (the grain F_8 has a visible 10-µm-thick bright outermost zone which was too thin to measure). Grains F_15 and F_17 had rims thick enough to be measured twice and showed that these rims have the same composition as the magmatic grains (Figs. 5 and 6). The remaining grains
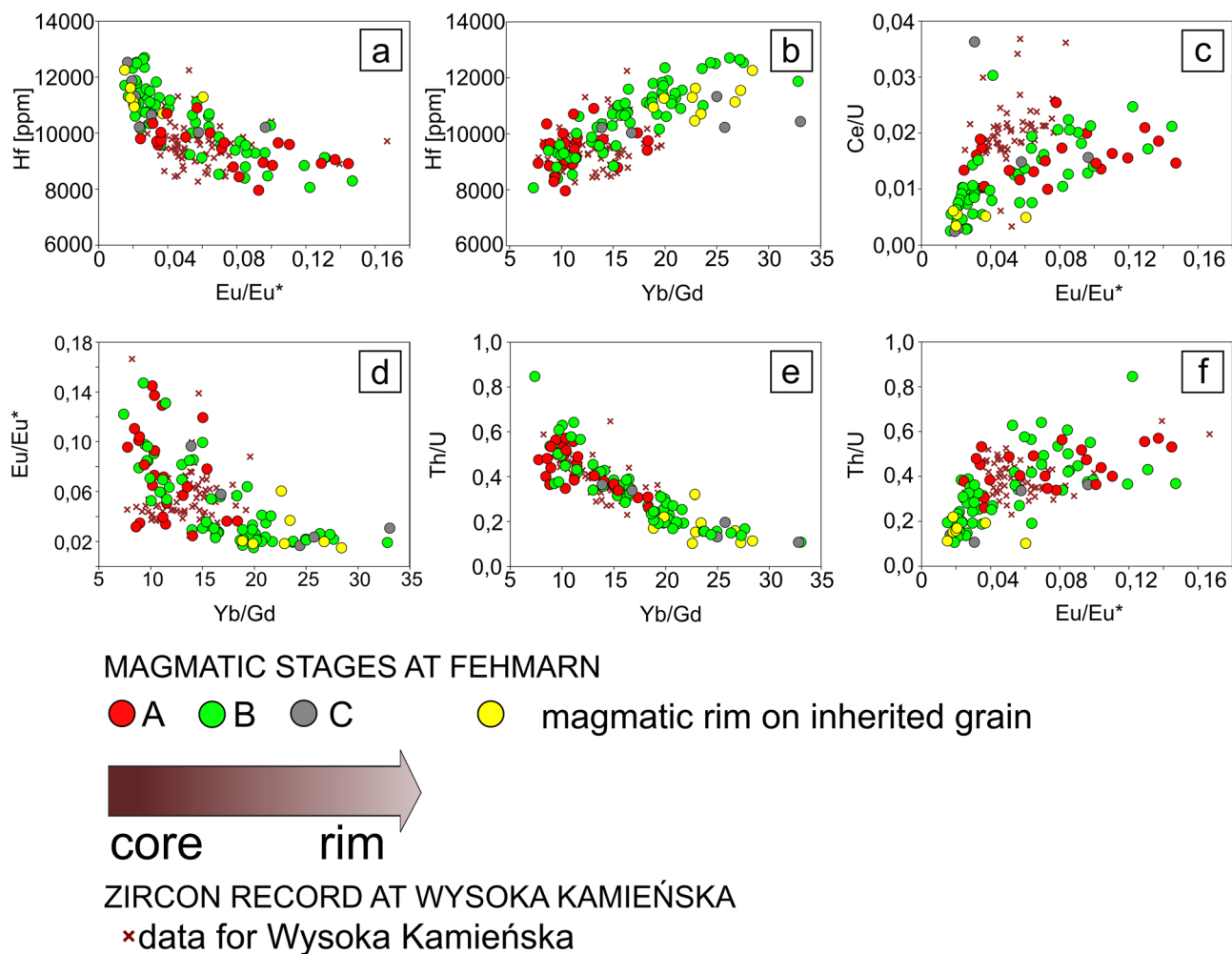
Fig. 6 Trace element compositions of magmatic zircon from Fehmarn along with the data for magmatic rims on inherited grains. Crosses correspond to Wysoka Kamieńska magmatic zircon

(n = 2 have a single analysis per grain with a composition typical of the rim composition (Fig. 6a–f).

Zircon from Wysoka Kamieńska

We analyzed 10 zircon grains which were magmatic. The general absence/low number of inherited zircon from this locality in this and previous studies needs to be highlighted (Breitkreuz et al. 2007 with only magmatic zircon, n = 18; Słodczyk et al. 2018 with magmatic zircon n = 16 and one older grain of 356 Ma). All these magmatic zircon grains are characterized by a generally lower and more restricted Hf concentration (8000–11,000 ppm) compared to other localities (Fig. 6a–f; SM 3). All measurements for Wysoka Kamieńska zircon cluster tightly for the majority of analyzed trace elements and show no general correlation of Hf concentration with Eu/Eu* anomaly (< 0.1, Fig. 6a) and Th/U ratio (0.3–0.6). The only observed pattern is visible for Yb/

Gd (7–20) where the ratio increases with decreasing Th/U (Fig. 6e).

Zircon from Salzwedel

We analyzed 16 zircon grains of which 11 were inherited with magmatic rims. Five magmatic zircon grains have the following ranges in composition: Hf (9000–13,000 ppm), Eu/Eu* < 0.09, Th/U (0.2–0.6), Yb/Gd (8—20), Ce/U < 0.02, Nd/Lu (0.02–0.08), Sm/Yb (~ 0.01–0.025) with different ranges representing core and rim sections (Fig. 9a–f; SM 4). Zircon isotopic composition was measured in one core ($\delta^{18}O$ = 8.1 ‰ and εHf of – 5.5), and several rims (7.7–9.4 ‰ and – 7.7 to – 5.5, respectively; Fig. 7). The rims show isotopic trends of decreasing $\delta^{18}O$ and increasing εHf with the increase in Hf concentration towards the outermost rims (Fig. 7). Inherited zircon grains have ages of 2104 Ma, 1564 Ma, 1440 Ma,
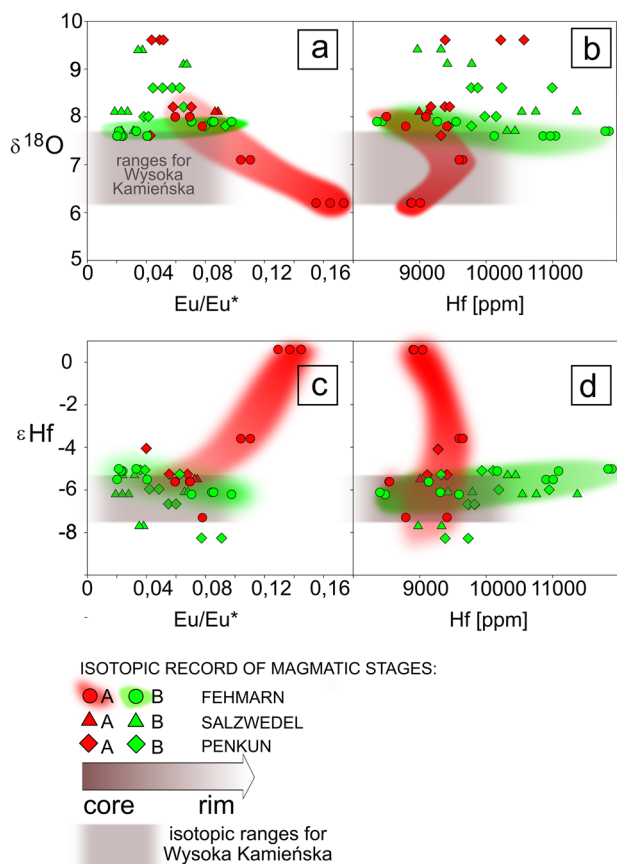
Fig. 7 Oxygen and Hf isotopic composition of cores and rims (based on the location within individual grains and corresponding Hf concentration pattern) with respect to magma differentiation indices such as Hf concentration and Eu/Eu*, Yb/Gd and Th/U ratios. Fehmarn, Salzwedel and Penkun isotopic data from Pietranik et al. (2013); Wysoka Kamieńska isotopic ranges (shadowed field) from Słodczyk et al. (2018)

1394 Ma, 1183 Ma, 982 Ma, 815 Ma, 800 Ma, 774 Ma, and 332 Ma ($n = 10$; data from Breitkreuz et al. 2007; for summary see also Table 1). One grain (S_14) has a magmatic rim dated at 294 Ma with no core measurements, however, its CL imaging and increased Eu/Eu* composition show a similarity to the inherited zircon group. Based on these observations, we included this grain in the inherited zircon group. Generally, the inherited zircon group in Salzwedel overlaps with the composition of inherited grains in Fehmarn (Fig. 8). Magmatic rims on inherited zircon grains were detected on all 11 grains, and eight of them have a composition typical for the rims in magmatic grains (Figs. 5 and 9a-f). The remaining three rims were too thin to perform analyses. For this locality, some analyses were excluded as they represented mixed inherited-and-magmatic trace element composition (e.g. S_1, S_4, S_8, S_10, S_15, and S_16; an example of boundary layer marked on Figs. 4d and 9).

Zircon from Penkun

We analyzed 18 zircon grains of which 6 were inherited with magmatic rims of variable thickness. The other 12 magmatic zircon grains show the following ranges of concentration for Hf (from 9 000 to 13 000 ppm); Eu/Eu* < 0.1, Th/U (0.2–0.8), Yb/Gd (8–25), Ce/U < 0.25, Nd/Lu < 0.08, Sm/Yb (0.005—0.025), with different ranges representing core and rim section (Fig. 10a–f; SM 5). Oxygen and Hf isotopic composition of cores show a spread in $\delta^{18}O$ from 9.6 to 7.6‰, while for εHf from – 4.1 to – 5.3. On the other hand, rims have $\delta^{18}O$ values from 7.6 to 8.6 ‰, and εHf from – 8.3 to – 5.3 (Fig. 7). Four inherited zircon grains have ages of 1793 Ma, 1464 Ma, 567 Ma, 355 Ma (Breitkreuz et al. 2007). Two grains (Pe_5 and Pe_9) have magmatic rim ages of 305 and 299 Ma, respectively with no core measurements, again their internal structure and high trace element ratios (e.g. Eu/Eu*; Th/U, Ce/U) show similarity to the inherited zircon group and were therefore included in the inherited zircon group. Generally, the inherited grains have a similar trace element composition to the grains in other localities with the exception of the 567 My grain (Pe_15) showing distinctly higher Eu/Eu* and lower Hf values (Fig. 8). Magmatic rims on inherited zircon were detected on 5 of the 6 grains. The rim on grain Pe_15 was too thin to measure (but it was still visible in the CL image; see SM 5). The magmatic rims on the remaining grains have Hf concentrations between 10,000 and 14,500 ppm. The majority of the rims fit within the outer rim composition except for one grain (Pe_11), which has a higher Eu/Eu* ratio (0.21—0.26) corresponding to the composition of inherited cores from this sample (probably due to the measurements performed in mixed zones).

Discussion

Rhyolitic magma evolution in the NE German Basin and NW Polish Basin

Zircon is a good indicator of rhyolitic magma evolution and preserves information on silicic magma formation in deeper magma reservoirs before an eruptible magma chamber is formed in the upper crust (e.g. Sliwinski et al. 2019; Szymanowski et al. 2017, 2019), and in younger zircon, it was shown that it may record secular compositional evolution from one eruption to another (Strom et al. 2014). The studied rhyolites were chosen because they had different Hf and O isotope compositions and corresponding differences in trace elements were expected. However, the trace element patterns have been shown to mostly overlap between localities and the same is true for the trace element compositions of inherited grains. Thus, despite the magmatic eruptions

Fig. 8 Trace element magma differentiation indices (Hf concentration, Eu/Eu*, Yb/Gd and Th/U ratios, respectively) versus age of inherited zircon grains from Fehmarn, Penkun and Salzwedel
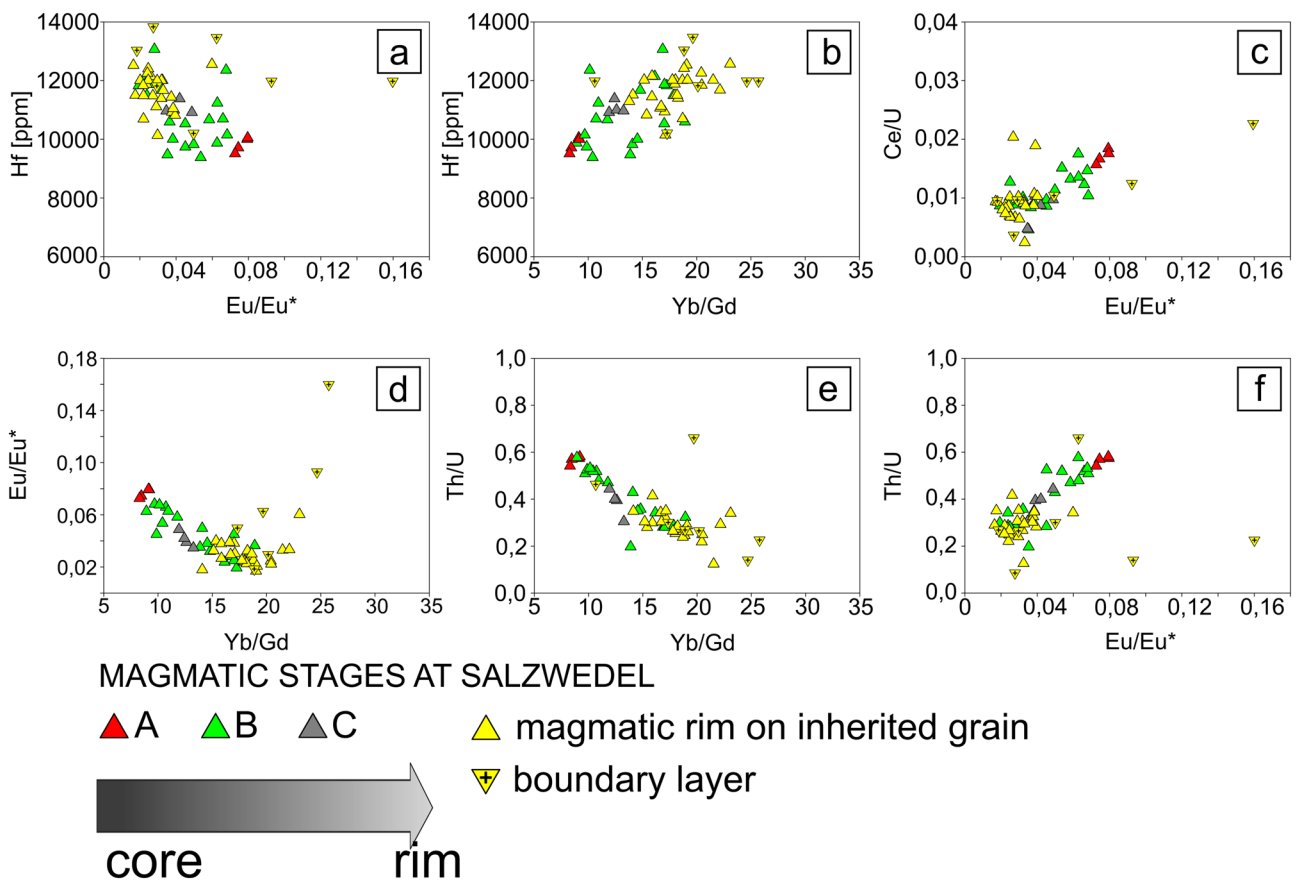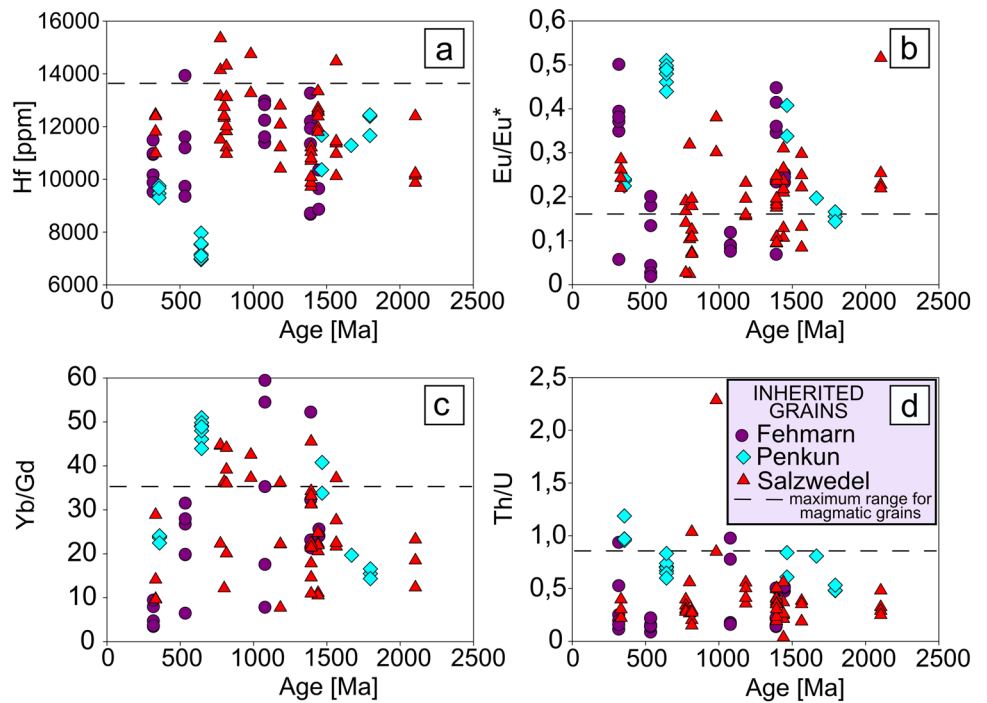

Fig. 9 Trace element compositions of magmatic zircon from Salzwedel along with the data for magmatic rims on inherited grains including data from boundary layers
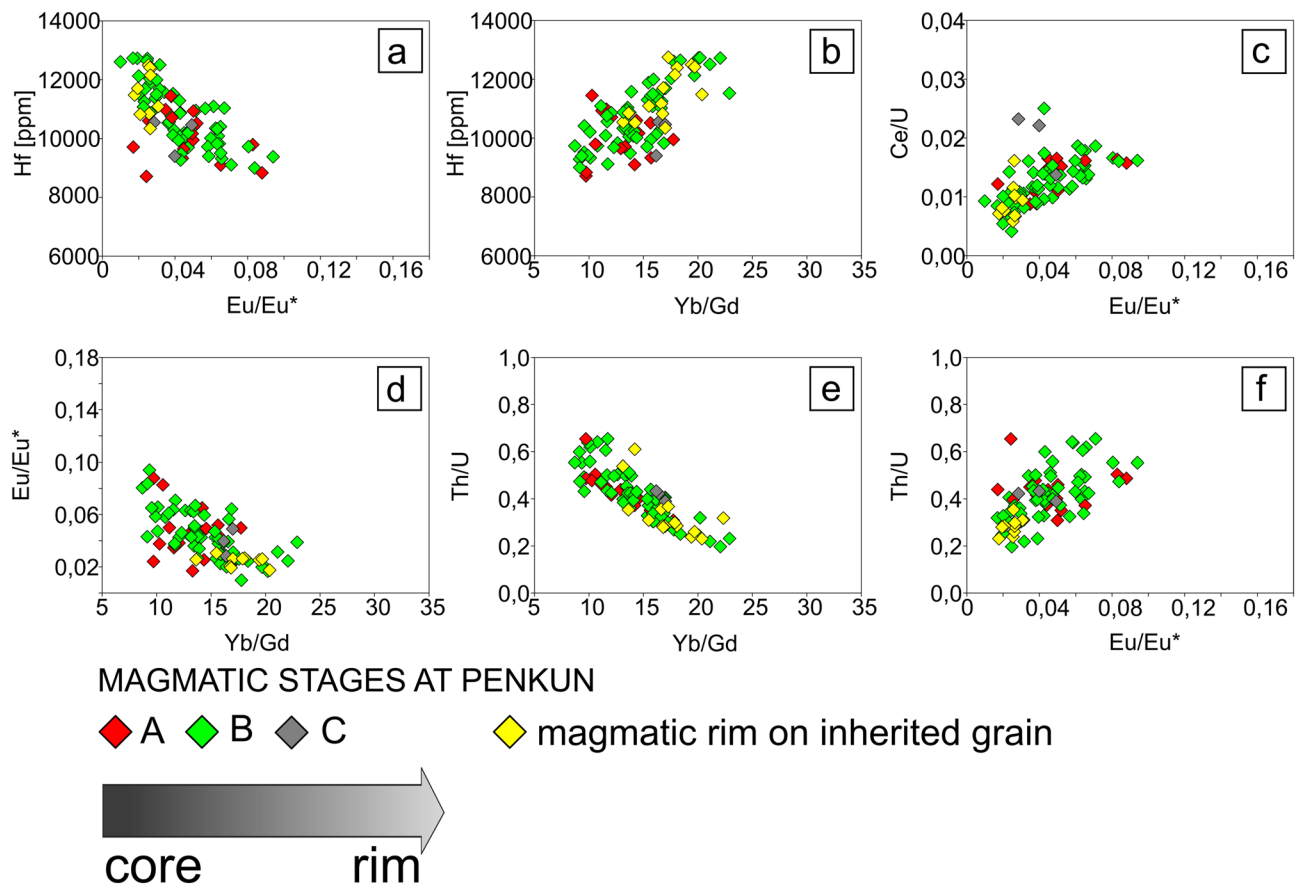
Fig. 10 Trace element compositions of magmatic zircon from Penkun along with the data for magmatic rims on inherited grains

investigated in this paper being several million years apart (see Table 1), they show similarities in potential sources and to some extent magma evolution processes. The trace element compositions can be generalized and correlated between grains for the NE German Basin localities and from this, three stages of magma evolution can be identified: stage A is recognized by the formation of the core region of some grains characterized by constant, rather low Hf concentration followed by its decrease. This pattern is reversed for the Th/U ratio, while Eu/Eu* shows a rather constant, but relatively high Eu/Eu* ratio; stage B is recognized by an increasing Hf concentration and Yb/Gd ratio accompanied by a decreasing Th/U ratio. The Eu/Eu* ratio is decreasing with respect to that observed in stage A; stage C is recognized by a shift in Hf concentration from a continuous increase in stage C to its flatting out or slight decrease within the rim region. More restricted zircon composition (corresponding to the A stage only) was typical of Wysoka Kamieńska (NW Polish Basin). These stages can be further interpreted in terms of rhyolitic magma evolution:

Stage A is typical of Fehmarn, Salzwedel, Penkun and Wysoka Kamieńska sites: where the zircon crystallized during stage A, i.e. before a marked increase in Hf

concentration, which shows some chemical variability between grains and locations, but less than the range of compositions observed in zircon crystallized during the later stage B. This may reflect crystallization from magma not affected by differentiation. The decrease in Hf noted in some grains at the end of stage A is correlated with an increase in Eu/Eu* and Th/U and a decrease in Yb/Gd. All these ratios can be interpreted in terms of rejuvenation with a less evolved magma (because a high Eu/Eu* ratio records the composition of a magma affected by less plagioclase fractionation and a low Yb/Gd ratio records less amphibole, clinopyroxene or titanite fractionation). Overlapping compositions are observed in the localities from the NE German Basin. In contrast, Wysoka Kamieńska shows mostly higher Ce/U ratios at given Eu/Eu* values compared to other localities (Fig. 6c), which may reflect more oxidized conditions. Further stages are not recorded in the Wysoka Kamieńska zircons; this suggests that Wysoka Kamieńska's magmatic system represents an early system that erupted before undergoing a prominent evolution path. As a consequence, stage A can be interpreted as a fingerprint of early zircon crystallization, followed by the addition of a more primitive magma pulse to the system.

Stage B is typical of only the Fehmarn, Salzwedel and Penkun sites: the compositional record is rather simple for this stage as an increasing Hf concentration in a rimward direction is accompanied by a decrease in the Eu/Eu*, Th/U and Ce/U ratios and an increase in Yb/Gd. The trends distinguished for A and early B stages overlap and cannot be detected based on scatter plots for trace elements or ratios (Fig. 11). Only detailed analyses of grain by grain individual patterns (Fig. 4 and SM 2–5) show that the trends go in opposite directions if moving from core to rim. That is why we suggest rejuvenation for stage A and continuous crystallization of zircon together with other major and accessory phases for stage B (Ballard et al. 2002; Burnham and Berry 2012; Trail et al. 2012; Deering et al. 2016; Large et al. 2018). Correlation between Eu/Eu* and Ce/U may also indicate a general trend of decreasing oxygen fugacity as a magma crystallizes zircon (Figs. 6c, 9c, 10c). The record is generally similar between all three analyzed localities, however, Fehmarn zircons have the widest range of observed compositions, with a generally more scattered pattern compared to the tight compositional fields observed for Salzwedel and Penkun (Fig. 11). This may indicate that Fehmarn is affected by more complex changes in both chemical melt evolution and oxygen fugacity which may be consistent with a higher input of less evolved (and more oxidized) magma at the later stages A for this locality. Therefore, stage B can be understood as a record of simple cooling of the system and continuous fractional crystallization, which seems to be more prolonged and complex at Fehmarn.

Stage C is again typical of only the Fehmarn, Salzwedel and Penkun sites: the record of this stage is relatively short and variable from grain to grain. The outermost rim may show a flattening of the trends observed in stage B or even their reversal. This stage is not easily detected in scatter plots, because it overlaps with the late stage B composition and again requires careful grain by grain observations in a core to rim direction. This last stage may reflect crystallization in a multiply saturated system, but it may also reflect a late recharge of the system with a less evolved magma, probably due to a rejuvenation event leading to crystal mush remobilization. The idea of mush remobilization leading to an eruption is a common scenario suggested for many volcanic systems (Bachmann and Bergantz 2008; Andersen et al. 2019; Tavazzani et al. 2020). As such, stage C may be interpreted as the result of the system reacting to the addition of a less fractionated portion of magma.

The implication coming from these detailed trace element analyses is that zircon may record processes of rejuvenation and fractional crystallization as well as the crystallization of zircon in a magmatic system over time, be it prolonged as at Fehmarn (and less so for Penkun and Salzwedel) or relatively short as at Wysoka Kamieńska. This may therefore be a potential tool to compare timescales of magma system evolution across a region such as the Central European Magmatic Province. Furthermore, we agree that the addition of thermal constraints would be a great asset to this and that is work for future analyses with Ti-in-zircon and Ti-in-quartz as possible thermometers.

Trace elements vs O and Hf isotopic composition in magmatic zircon

It is accepted that rhyolitic magmas form either by partial melting of the crust, fractional crystallization of more mafic
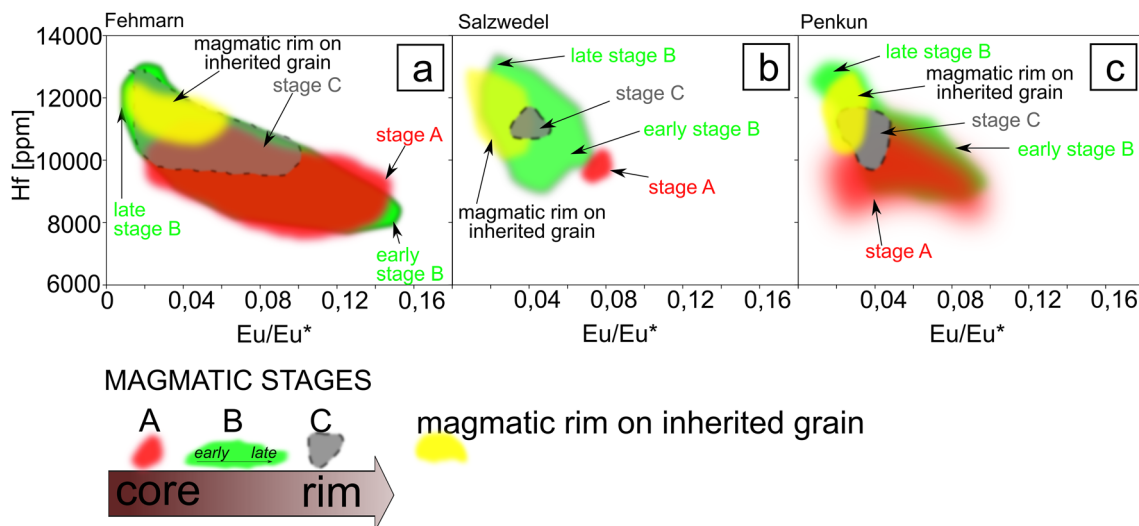

Fig. 11 Compositional fields for magmatic stages A, B, and C with respect to the composition of the magmatic rim on inherited zircon grains for: **a** Fehmarn, **b** Salzwedel, **c** Penkun. Stage B is marked as one field, but the direction from early to late (i.e. rim ward) is shown. Wysoka Kamieńska is not shown, as it does not contain any inherited grains

magmas, or a combination of these factors (e.g. Charlier et al. 2008; Sliwinski et al. 2019; Yan et al. 2020; Tavazzani et al. 2020; Lukács et al. 2021). It is also accepted that combined isotopic and trace element analyses may distinguish between magma differentiation dominated by fractional crystallization or by assimilation of crustal melts. Also, rejuvenation by more primitive magmas should be detected. Thus in this study, we used zircons with known O and Hf isotopic composition that were previously interpreted as a record of a coalescence of chemically variable magmas (representing different proportions of crustal melting versus primitive magma fractionation in the source region) followed by homogenization (Pietranik et al. 2013). Direct correlation between the trace element measurements and isotope analyses is not possible, because of the difference in the analytical spot size, but the isotopic composition can be correlated roughly to stages A or B (Fig. 7), stage C was not analyzed isotopically. A clear low δ^{18}O and high εHf value are observed for two grains in Fehmarn, and these values are correlated with the change in trace element composition towards a more primitive value (increasing Eu/Eu*, and decreasing Hf). However, stage A generally records a large spread in isotopic values. This may be consistent with either (a) a coalescence of isotopically variable magmas as proposed by Pietranik et al. (2013) or (b) variable mixing between a primitive magma joining the magmatic system at the later stages of A and a more crustal-like magma. The two processes are not exclusive. If mixing was responsible for the primitive isotopic values observed at Fehmarn it may indicate that this locality was more affected by this early rejuvenation. A potentially higher proportion of primitive magma at Fehmarn is not clearly reflected in the trace element content in the zircon (as they overlap between localities), but may be consistent with (a) a lack of high δ^{18}O and low εHf values in stage B zircon, when such values are observed at Salzwedel and Penkun, (b) a wider compositional change observed within the grains, suggesting longer crystallization perhaps in a hotter magma, (c) or more thorough isotopic homogenization evident in the homogeneous composition of zircon crystallized at stage B. More crustal-like isotopic values occur in zircon from Penkun and Salzwedel, but they steadily move towards more primitive values as the magma fractionates during stage B. This may reflect a higher proportion of crustal magma that evolves towards a more mixed, homogenous composition as it fractionates. Wysoka Kamieńska records the shortest time span of crystallization as suggested by the presence of the most restricted zircon compositions representing only stage A. The zircons in this location have low variability in δ^{18}O and εHf isotopic composition (ranges from these rhyolites are marked on Fig. 7). Moreover, the zircon does not show high Eu/Eu* values and no Eu/Eu* vs Hf trend. The lower Eu/Eu* values at Wysoka Kamieńska as compared to other

localities may be explained by general zircon crystallization after more intense fractionation of feldspar and thus resulted in inheritance of lower Eu/Eu* values from the surrounding melt. The lack of a trend between Eu/Eu* vs Hf may be explained by the relatively quick crystallization of zircon that did not record melt evolution along with cooling of the system, probably due to its rapid remobilization and eruption. Altogether it is clear that combined isotope and trace element analyses may provide more information on the evolution of these rhyolitic systems. However, not all processes are recorded in the same way in those analytical approaches. For example, early rejuvenation is only scarcely recorded in the isotopic composition of a few grains, whereas the trace element record is preserved in the majority of grains. However, this may be due to the generally better resolution of trace element analyses but underlines the importance of using both methods.

## Magma recharge—when did the older zircon join the magma?

Melting of the continental crust produces magmas that are considered an important source of rhyolites. Partial melting of the crust might be caused by either the direct intrusion of magma from the mantle (low-degree production of partial melt) or by thermal rejuvenation caused by heat released from frequent basaltic intrusions at shallow depths (increased-degree of produced partial melt; e.g. Szymanowski et al. 2017, 2019; Tavazzani et al. 2020). The record of partial melting, if not obliterated by subsequent processes of mixing with more primitive, mantle-derived magmas, may be detected via mineral dissolution/resorption textures and/or the lack of equilibrium between coexisting crystals and melt (as for the Krafla volcano, where—following the drilling project—these features were observed in situ; Masotta et al. 2018). Inherited zircon is a prime example of a mineral that survives partial melting and is often considered as representing the crustal source of rhyolitic magmas. However, it is not always clear if the inherited zircon represents the source or if it was added from the wall rock into the magma during its evolution that was dominated by assimilation–fractional crystallization process.

In this study, we suggest that important information relating to silicic magma crystallization can be obtained by studying the composition of magmatic rims on inherited zircon grains and compare it to that of fully magmatic grains. First of all, the presence versus absence of inherited grains needs to be discussed. Wysoka Kamieńska—this site is characterized by a small number of inherited zircon (Breitkreuz et al. 2007; Słodczyk et al. 2018). Based on the isotopic composition of these zircon, Słodczyk et al. (2018) suggested that the rhyolites were derived from the melting of fine-grained sedimentary material (an Avalonian accretionary prism) mixed

with volumetrically dominating mantle-derived magmas. In contrast, the Fehmarn, Penkun, and Salzwedel sites contain variable proportions of magmatic and inherited grains (Breitkreuz et al. 2007), suggesting, at the first approach, that the crustal source material was rich in zircon. However, this conclusion is not supported by the present study as all rims on the inherited grains show the same magmatic trace element composition which is consistent with crystallization during late stage B and thus refers to the similar late timing of the recharge event (Fig. 11) and similar residence times within the magma systems before their evacuation and eruption. The thickness of the magmatic rims do vary, but the maximum widths are similar between localities i.e. 60 μm for Salzwedel, 50 μm for Fehmarn, and 65 μm for Penkun. Estimated zircon growth rates vary between 10^{-11} and 10^{-14} cm/s (Schmitt et al. 2011; Bindeman and Melnik 2016; Zhang and Xu 2016). Therefore, the rims needed somewhere between a few years to thousands of years to crystallize. This time span should therefore approximately mark a period of magma homogenization and final rejuvenation, which took place after the first recorded rejuvenation during stage A and subsequent assimilation-fractional crystallization during

early stage B (Fig. 12). It could be that material assimilated during stage B provided the inherited grains, but there was a time lag before they resumed crystallization. Regardless of if the inherited zircon grains were assimilated during stage B or not, they do not represent an early crustal source from which the rhyolite magmas were derived. There are two possible explanations for this observation: (1) the initial rhyolitic magmas were too hot and zircon undersaturated and the zircon from the source is therefore fully dissolved or (2) the first stages recorded in the zircon represent differentiated mafic magmas and the addition of crustal melts would be later. However, relatively high $\delta^{18}O$ and low εHf values for zircon crystallized during stage A is more consistent with the first explanation. This interpretation is further supported by the lack of inherited zircon in Wysoka Kamieńska, which records only the early stages of zircon crystallization (Fig. 12). The first major implication of this is that the lack of inherited zircon is less source-dependent and more marks a certain evolution path of rhyolitic magma i.e. rhyolites that underwent short evolution and quick eruption would not contain inherited zircon. The second interpretation is that perhaps only rarely we can find zircon representing the

Fig. 12 Schematic model of the magma evolution based on zircon trace element and isotopic composition record
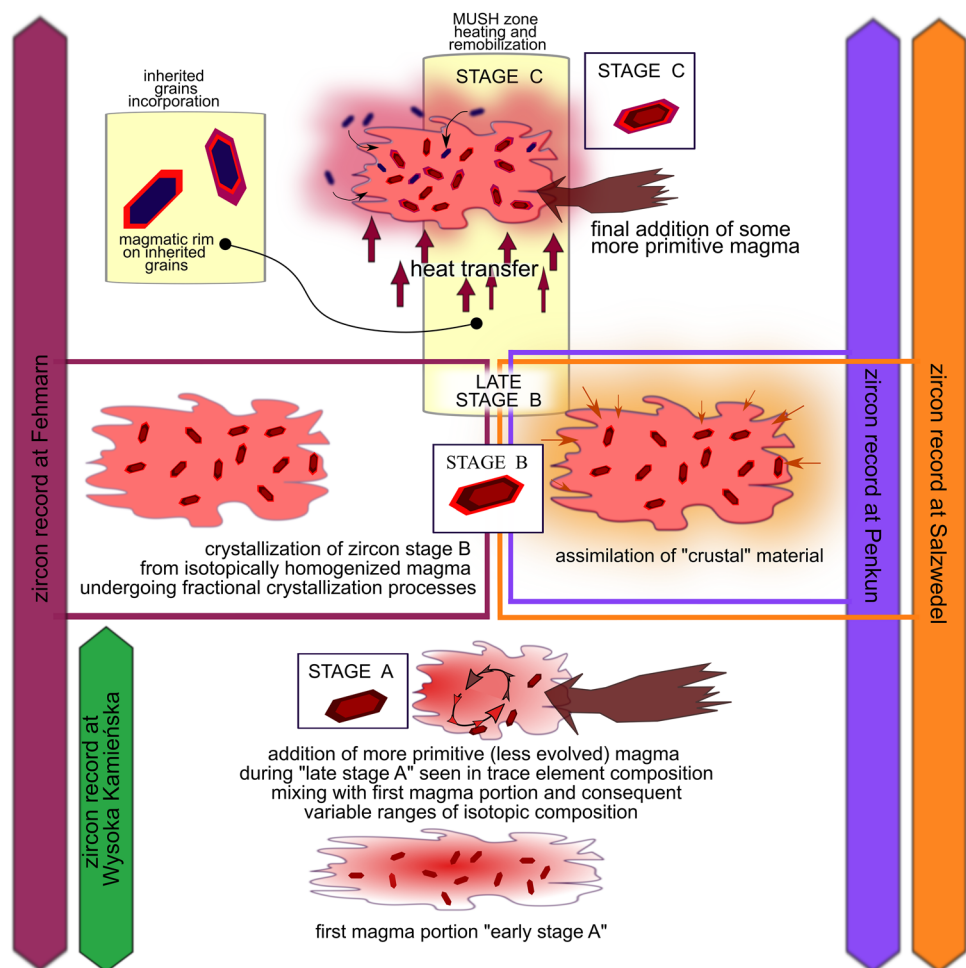
initial source and thus what we analyzed in the inherited zircon is upper crustal material where rhyolitic magmas reside before their final emplacement and eruption.

Conclusions

Zircon core-to-rim trace element composition and differentiation indices can be used to identify magmatic stages reflecting magma evolution through fractionation, assimilation, and/or recharge with more primitive melts. New information is obtained when such a record is interpreted along with O and Hf isotopic compositions. Our results from this study show that zircon from the NE German Basin (Fehmarn, Salzwedel, and Penkun sites) records early evolution from a magma affected by common recharge, followed by prolonged fractional crystallization indicating a high degree of magma maturation within a long-lived magmatic system. The magmas at Salzwedel and Penkun were also experiencing assimilation during this stage. The Fehmarn magma was also assimilating material, but the trace element and isotope records are overshadowed by more intense magma recharge. Lastly, all three localities may have recorded recharge during the late magmatic stages. Interestingly, the inherited grains from these localities have rim compositions overlapping only with strongly fractionated compositions (late stage B; Fig. 11) suggesting that the majority of the inherited zircon was incorporated during assimilation and not from the crustal source of the magmas. Inherited zircon grains are very rare at Wysoka Kamieńska (NW Polish Basin) indicating less fractionated magma was involved, supporting the absence of later stages when the majority of inherited zircons would join the melt (Fig. 12). This might be generally explained by a short residence time following rejuvenation within the magma chamber and rapid evacuation of hotter, less evolved melts. Altogether, a juxtaposition of isotopic and trace element data reveals more details on magma evolution by contemporaneous fractional crystallization, assimilation, and rejuvenation of the system by varied magma portions i.e. of mafic (less evolved) origin as for Fehmarn, or crustal (more evolved) associations for Salzwedel and Penkun. The comparison of chemical and isotopic trends between different parts of the crystals gives a complementary record, but the better resolution of trace element data reveals important details of magma evolution, which were not recorded by isotopes such as early and late rejuvenation. Lastly, only detailed grain-by-grain analyses in core-to-rim directions reveal information on successive stages of magma evolution as the composition of respective stages may overlap in scatter plots.

References

Anders E, Grevesse N (1989) Abundances of the elements: meteoritic and solar. Geochim Cosmochim Acta 53:197–214. https://doi.org/10.1016/0016-7037(89)90286-X

Andersen NL, Singer BS, Coble MA (2019) Repeated rhyolite eruption from heterogeneous hot zones embedded within a cool, shallow magma reservoir. Geophys Res Solid Earth 124:2582–2600. https://doi.org/10.1029/2018JB016418

Bachmann O, Bergantz GW (2008) Rhyolites and their source mushes across tectonic settings. J Petrol 49:2277–2285. https://doi.org/10.1093/petrology/egn068

Ballard JR, Palin MJ, Campbell IH (2002) Relative oxidation states of magmas inferred from Ce (IV)/Ce (III) in zircon: application to porphyry copper deposits of northern Chile. Contrib Mineral Pet 144:347–364. https://doi.org/10.1007/s00410-002-0402-5

Benek R, Kramer W et al (1996) Permo-carboniferous magmatism of the Northeast German Basin. Tectonophysics 266:379–404. https://doi.org/10.1016/S0040-1951(96)00199-0

Bindeman IN, Melnik OE (2016) Zircon survival, rebirth and recycling during crustal melting, magma crystallization, and mixing based on numerical modelling. J Pet 57:437–460. https://doi.org/10.1093/petrology/egw013

Bindeman IN, Fu B, Kita NT, Valley JW (2008) Origin and evolution of silicic magmatism at Yellowstone based on ion microprobe analysis of isotopically zoned zircons. J Petrol 49:163–193. https://doi.org/10.1093/petrology/egm075

Breitkreuz C, Kennedy A (1999) Magmatic flare-up at the Carboniferous/Permian boundary in the NE German Basin revealed by SHRIMP zircon ages. Tectonophysics 302:307–326. https://doi.org/10.1016/S0040-1951(98)00293-5

Breitkreuz C, Kennedy A, Geißler M, Ehling BC, Kopp J, Muszynski A, Stouge S (2007) Far Eastern Avalonia: Its chronostratigraphic structure revealed by SHRIMP zircon ages from Upper Carboniferous to Lower Permian volcanic rocks (drill cores from Germany, Poland, and Denmark). Geol Soc Am Spec Pap 423:173–190. https://doi.org/10.1130/2007.2423(07)

Burnham AD, Berry AJ (2012) An experimental study of trace element partitioning between zircon and melt as a function of oxygen

fugacity. Geochim Cosmochim Acta 95:196–212. https://doi.org/10.1016/j.gca.2012.07.034

Casas-García R, Rapprich V, Breitkreuz C, Svojtka M, Lapp M, Stanek K, Linnemann U (2019) Lithofacies architecture, composition, and age of the Carboniferous Teplice Rhyolite (German–Czech border): Insights into the evolution of the Altenberg-Teplice Caldera. J Volcanol Geotherm Res 386:106662. https://doi.org/10.1016/j.jvolgeores.2019.106662

Casas-García R, Rapprich V, Repstock A, Magna T, Schulz B, Kochergina Y, Breitkreuz C (2021) Crustal vs. mantle contributions in the Erzgebirge/Krušné hory Mts .magmatism: Implications for generation of zoned, A-type silicic rocks in the late-Variscan Altenberg-Teplice Caldera, Central Europe. Lithos 404:106429. https://doi.org/10.1016/j.lithos.2021.106429

Charlier BL, Wilson CJ, Davidson JP (2008) Rapid open-system assembly of a large silicic magma body: time-resolved evidence from cored plagioclase crystals in the Oruanui eruption deposits, New Zealand. Contrib Mineral Pet 156:799–813. https://doi.org/10.1007/s00410-008-0316-y

Dadlez R (2006) The Polish Basin—relationship between the crystalline, consolidated and sedimentary crust. Geol Q 50:43–58

Deering D, Keller B, Schoene B, Bachmann O, Beane R, Ovtcharova M (2016) Zircon record of the plutonic-volcanic connection and protracted rhyolite melt evolution. Geology 44:267–270. https://doi.org/10.1130/G37539.1

Geißler M, Breitkreuz C, Kiersnowski H (2008) Late Paleozoic volcanism in the central part of the Southern Permian Basin (NE Germany, W Poland): facies distribution and volcano-topographic hiati. Int J Earth Sci 97:973–989. https://doi.org/10.1007/s00531-007-0288-6

Hübner M, Breitkreuz C, Repstock A, Schulz B, Pietranik A, Lapp M, Heuer F (2021) Evolution of the Lower Permian Rochlitz volcanic system, Eastern Germany: reconstruction of an intracontinental supereruption. Int J Earth Sci 110:1995–2020. https://doi.org/10.1007/s00531-021-02053-5

Jackowicz E (1995) Lower Rotliegend volcanic rocks from the western part of the Polish Lowland. Terra Nostra 7:67–69

Karnkowski PH (1999) Origin and evolution of the Polish Rotliegend Basin. Pol Geol Inst Spec Pap 3:1–93

Kemp A, Hawkesworth C, Foster G, Paterson B, Woodhead J, Hergt J, Gray C, Whitehouse M (2007) Magmatic and crustal differentiation history of granitic rocks from Hf–O isotopes in zircon. Science 315:980–983. https://doi.org/10.1126/science.1136154

Large SJ, Quadt AV, Wotzlaw JF, Guillong M, Heinrich CA (2018) Magma evolution leading to porphyry Au-Cu mineralization at the Ok Tedi deposit, Papua New Guinea: Trace element geochemistry and high-precision geochronology of igneous zircon. Econ Geol 113:39–61. https://doi.org/10.5382/econgeo.2018.4543

Lukács R, Guillong M, Bachmann O, Fodor L, Harangi S (2021) Tephrostratigraphy and magma evolution based on combined zircon trace element and U-Pb age data: fingerprinting Miocene silicic pyroclastic rocks in the Pannonian Basin. Front Earth Sci 9:615768. https://doi.org/10.3389/feart.2021.615768

Maliszewska A, Jackowicz E, Kuberska M, Kiersnowski H (2016) Lower Permian (Rotliegend) rocks of western Poland–A petrographic monograph. Pr Państwowego Inst Geol 204:1–113

Masotta M, Mollo S, Nazzari M, Tecchiato V, Scarlato P, Papale P, Bachmann O (2018) Crystallization and partial melting of rhyolite and felsite rocks at Krafla volcano: a comparative approach based on mineral and glass chemistry of natural and experimental products. Chem Geol 483:603–618

McCann T, Pascal C et al (2006) Post-Variscan (end Carboniferous-Early Permian) basin evolution in western and central Europe. Geol Soc Lond Memoirs 32:355–388. https://doi.org/10.1144/GSL.MEM.2006.032.01.22

Mock A, Jerram DA, Breitkreuz C (2003) Using quantitative textural analysis to understand the emplacement of shallow-level rhyolitic laccoliths—a case study from the Halle Volcanic Complex, Germany. J Pet 44:833–849. https://doi.org/10.1093/petrology/44.5.833

Paulick H, Breitkreuz C (2005) The Late Paleozoic felsic lava-dominated large igneous province in northeast Germany: volcanic facies analysis based on drill cores. Int J Earth Sci 94:834–850. https://doi.org/10.1007/s00531-005-0017-y

Pietranik A, Słodczyk E, Hawkesworth CJ, Breitkreuz C, Storey CD, Whitehouse M, Milke R (2013) Heterogeneous zircon cargo in voluminous Late Paleozoic rhyolites: Hf, O isotope and Zr/Hf records of plutonic to volcanic magma evolution. J Pet 54:1483–1501. https://doi.org/10.1093/petrology/egt019

Reid MR, Vazquez JA (2017) Fitful and protracted magma assembly leading to a giant eruption, Youngest Toba Tuff, Indonesia. Geochem Geophys Geosyst 18:156–177. https://doi.org/10.1002/2016GC006641

Repstock A, Breitkreuz C, Lapp M, Schulz B (2018) Voluminous and crystal-rich igneous rocks of the Permian Wurzen volcanic system, northern Saxony, Germany: physical volcanology and geochemical characterization. Int J Earth Sci 107:1485–1513. https://doi.org/10.1007/s00531-017-1554-x

Rivera TA, Schmitz MD, CrowleyJL SM (2014) Rapid magma evolution constrained by zircon petrochronology and 40Ar/39Ar sanidine ages for the Huckleberry Ridge Tuff, Yellowstone, USA. Geology 42:643–646. https://doi.org/10.1130/G35808.1

Schmiedel T, Breitkreuz C, Görz I, Ehling BC (2015) Geometry of laccolith margins: 2D and 3D models of the Late Paleozoic Halle Volcanic Complex (Germany). Int J Earth Sci 104:323–333. https://doi.org/10.1007/s00531-014-1085-7

Schmitt AK, Danišík M, Evans NJ, Siebel W, Kiemele E, Aydin F, Harvey JC (2011) Acigöl rhyolite field, Central Anatolia (part 1): high-resolution dating of eruption episodes and zircon growth rates. Contrib Mineral Pet 162:1215–1231. https://doi.org/10.1007/s00410-011-0648-x

Sliwinski J, Farsky D, Lipman PW, Guillong M, Bachmann O (2019) Rapid magma generation or shared magmatic reservoir? Petrology and geochronology of the rat creek and nelson mountain tuffs, CO, USA. Front Earth Sci. https://doi.org/10.3389/feart.2019.00271

Słodczyk E, Pietranik A, Glynn S, Wiedenbeck M, Breitkreuz C, Dhuime B (2018) Contrasting sources of Late Paleozoic rhyolite magma in the Polish Lowlands: evidence from U-Pb ages and Hf and O isotope composition in zircon. Int J Earth Sci 107:2065–2081. https://doi.org/10.1007/s00531-018-1588-8

Stelten ME, Cooper KM, Vazquez JA, Calvert AT, Glessner JJ (2015) Mechanisms and timescales of generating eruptible rhyolitic magmas at Yellowstone caldera from zircon and sanidine geochronology and geochemistry. J Pet 56:1607–1642. https://doi.org/10.1093/petrology/egv047

Storm S, Schmitt AK et al (2014) Zircon trace element chemistry at sub-micrometer resolution for Tarawera volcano, New Zealand, and implications for rhyolite magma evolution. Contrib Mineral Pet 167:1000. https://doi.org/10.1007/s00410-014-1000-z

Szymanowski D, Wotzlaw JF, Ellis BS, Bachmann O, Guillong M, von Quadt A (2017) Protracted near-solidus storage and pre-eruptive rejuvenation of large magma reservoirs. Nat Geosci 10:777–782. https://doi.org/10.1038/ngeo3020

Szymanowski D, Ellis BS, Wotzlaw JF, Bachmann O (2019) Maturation and rejuvenation of a silicic magma reservoir: high-resolution chronology of the Kneeling Nun Tuff. Earth Planet Sci Lett 510:103–115. https://doi.org/10.1016/j.epsl.2019.01.007

Tavazzani L, Peres S, Sinigoi S, Demarchi G, Economos RC, Quick JE (2020) Timescales and mechanisms of crystal-mush rejuvenation and melt extraction recorded in Permian plutonic and volcanic

rocks of the Sesia magmatic system (Southern Alps, Italy). J Pet. https://doi.org/10.1093/petrology/egaa049

Trail D, Watson EB, Tailby ND (2012) Ce and Eu anomalies in zircon as proxies for the oxidation state of magmas. Geochim Cosmochim Acta 97:70–87. https://doi.org/10.1016/j.gca.2012.08.032

Valley JW, Lackey JS, Cavosie AJ, Clechenko CC, Spicuzza MJ, Basei MA et al (2005) 4.4 billion years of crustal maturation: oxygen isotope ratios of magmatic zircon. Contrib Mineral Petrol 150:561–580. https://doi.org/10.1007/s00410-005-0025-8

Van Achterbergh E, Ryan C, Jackson S, Griffin W (2001) Data reduction software for LA-ICP-MS. Mineralog Assoc Can 29:239–243

Van Wees JD, Stephenson RA, Ziegler PA, Bayer U, McCann T, Dadlez R, Scheck M (2000) On the origin of the southern Permian Basin, Central Europe. Mar Pet Geol 17:43–59. https://doi.org/10.1016/S0264-8172(99)00052-5

Yan LL, He ZY, Klemd R, Beier C, Xu XS (2020) Tracking crystal-melt segregation and magma recharge using zircon trace element data. Chem Geol 542:119596. https://doi.org/10.1016/j.chemgeo.2020.119596

Żelaźniewicz A, Oberc-Dziedzic T, Fanning CM, Protas A, Muszyński A (2016) Late Carboniferous–early Permian events in the Trans-European Suture Zone: tectonic and acid magmatic evidence from Poland. Tectonophysics 675:227–243. https://doi.org/10.1016/j.tecto.2016.02.040

Zhang Y, Xu Z (2016) Zircon saturation and Zr diffusion in rhyolitic melts, and zircon growth geospeedometer. Am Min 101:1252–1267. https://doi.org/10.2138/am-2016-5462

J Geophys Res Solid Earth 124: 2582–2600. https://doi.org/10.1029/2018JB016418